

Weak form factors for heavy meson decays: an update

D. Melikhov and B. Stech

ITP, Universität Heidelberg, Philosophenweg 16, D-69120, Heidelberg, Germany

We calculate the form factors for weak decays of $B_{(s)}$ and $D_{(s)}$ mesons to light pseudoscalar and vector mesons. To reveal the intimate connection between different decay modes and to be able to perform the calculations in the full physical q^2 -region we use a relativistic dispersion approach based on the constituent quark picture. This approach gives the form factors as relativistic double spectral representations in terms of the wave functions of the initial and final mesons. The form factors have the correct analytical properties and satisfy all general requirements of QCD in the heavy quark limit.

The disadvantages of quark models, such as ill-defined effective quark masses and not precisely known meson wave functions, are greatly diminished by fitting the quark model parameters to lattice QCD results for the $B \rightarrow \rho$ transition form factors at large momentum transfers and to the measured total $D \rightarrow (K, K^*)l\nu$ decay rates. This allows us to predict numerous form factors for all kinematically accessible q^2 values.

PACS numbers: 12.39.Ki, 13.20.He, 13.20.Fc

I. INTRODUCTION

The knowledge of the weak transition form factors of heavy mesons is crucial for a proper extraction of the quark mixing parameters, for the analysis of non-leptonic decays and CP violating effects and, related to it, for a search of New Physics.

Theoretical approaches for calculating these form factors are quark models [1–8], QCD sum rules [9–12], and lattice QCD [13]. Although in recent years considerable progress has been made, the theoretical uncertainties are still uncomfortably large. An accuracy better than 15% has not been attained. Moreover each of the above methods has only a limited range of applicability, namely:

QCD sum rules are suitable for describing the low q^2 region of the form factors. The higher q^2 region is hard to get and higher order calculations are not likely to give real progress because of the appearance of many new parameters. The accuracy of the method cannot be arbitrarily improved because of the necessity to isolate the contribution of the states of interest from others.

Lattice QCD gives good results for the high q^2 region. But because of the many numerical extrapolations involved this method does not provide for a full picture of the form factors and for the relations between the various decay channels.

Quark models do provide such relations and give the form factors in the full q^2 range. However, quark models are not closely related to the QCD Lagrangian (or at least this relationship is not well understood yet) and therefore have input parameters which are not directly measurable and may not be of fundamental significance.

In this situation it becomes evident that a combination of various methods will be fruitful. It is the purpose of this paper to obtain this way reliable predictions for many decay form factors in their full q^2 ranges.

To achieve this goal, one needs a general frame for the description of the large variety of processes. This can be only a suitable quark model, because only a quark model can connect different processes through the soft wave functions of the mesons and describes the full q^2 range of the form factors¹. The shortcomings of this model will be greatly diminished by incorporating the results from the more fundamental QCD based methods.

Historically, constituent quark models have been first to analyse the meson transition form factors. Although a rigorous derivation of this approach as an effective theory of QCD in the nonperturbative regime has not been obtained, relativistic quark models work surprisingly well for the description of the meson spectra and form factors. Moreover, constituent quark models provide so far the only operative method for dealing with excited states.

¹One of the first steps in combining various approaches in order to obtain predictions for the form factors for all q^2 has been done in [14] where a simple lattice-constrained parametrization based on the constituent quark picture of Ref. [15] and pole dominance has been proposed.

1. The physical picture

Constituent quark models are based on the following phenomena expected from QCD:

- i) chiral symmetry breaking in the low-energy region provides for the masses of the constituent quarks;
- ii) the strong peaking of the soft (nonperturbative) hadronic wave functions in terms of the quark momenta with a width of the order of the confinement scale; and
- iii) the dominance of Fock states with the minimal number of constituents, i.e. a $q\bar{q}$ composition of mesons.

An important shortcoming of previous quark model predictions was a strong dependence of the results on the special form of the quark model and on the parameter values.

The goal of this paper is to demonstrate that once (a) a proper relativistic formalism is used for the description of the transition form factors and (b) the numerical parameters of the model are chosen properly (we discuss criteria for such a proper choice below), the quark model yields results in full agreement with existing experimental data and in accord with the predictions of more fundamental theoretical approaches. In addition, our quark model allows to predict many other form factors which have not yet been measured.

2. The formalism

For the description of the transition form factors in their full q^2 range and for various initial and final mesons, a fully relativistic treatment is necessary. We therefore choose a formulation of the quark model which is based on the relativistic dispersion approach [16] and thus guarantees the correct spectral and analytical properties.

Within this model, the transition form factors are given by relativistic double spectral representations through the wave functions of the initial and final mesons both in the scattering and the decay regions. An important feature of the spectral representations of the transition form factors is that they respect all known rigorous theoretical constraints on the form factors. The form factors of the dispersion quark model have the correct heavy-quark expansion at leading and next-to-leading $1/m_Q$ orders in accordance with QCD for transitions between heavy quarks [17,18]. For the heavy-to-light transition the dispersion quark model satisfies the relations between the form factors of vector, axial-vector, and tensor currents valid at small recoil [19]. In the limit of the heavy-to-light transitions at small q^2 the form factors obey the lowest order $1/m_Q$ and $1/E$ relations of the Large Energy Effective Theory [20] and provide the pattern of higher-order symmetry-violating effects.

Another important advantage of the dispersion formulation of the quark model is the fact that one directly obtains the form factors in the physical decay region $q^2 > 0$. No numerical extrapolation from space-like values is required.

3. Parameters of the model

In previous applications of quark models the transition form factors turned out to be sensitive to the numerical parameters, such as the quark masses and the slopes of the meson wave functions. As proposed in Ref. [21], the way to control these parameters is to use the results of lattice calculations at large q^2 as 'experimental' inputs. In [22] the b and u constituent quark masses and slope parameters of the B , π , and ρ wave functions have been obtained through this procedure.

We now consider in addition the charm and strange mesons. To determine the charm and strange meson wave functions and the effective mass values m_c and m_s we use here as input the measured total rates for the decays $D \rightarrow (K, K^*)l\nu$. By fixing the parameters in this way we overcome the main uncertainties of the quark model calculations. This allows us to give numerous predictions for the form factors of the transitions of the heavy and strange heavy mesons D , D_s , B , and B_s into light mesons.

The paper is organized as follows. Section II briefly presents the main features of the double spectral representations of the form factors. In Section III we determine the numerical parameters of the model and give the predictions of the form factors. Section 4 contains our conclusions.

II. MESON TRANSITION FORM FACTORS

The long-distance contribution to meson decays is contained in the relativistic invariant transition form factors of the vector, axial-vector and tensor currents. The amplitudes of the $M_1 \rightarrow M_2$ transition induced by the weak $q_2 \rightarrow q_1$ quark transition through the vector $V_\mu = \bar{q}_1 \gamma_\mu q_2$, axial-vector $A_\mu = \bar{q}_1 \gamma_\mu \gamma^5 q_2$, tensor $T_{\mu\nu} = \bar{q}_1 \sigma_{\mu\nu} q_2$, and pseudotensor $T_{\mu\nu}^5 = \bar{q}_1 \sigma_{\mu\nu} \gamma^5 q_2$ currents, have the following covariant structure [19]

$$\begin{aligned}
\langle P(M_2, p_2) | V_\mu(0) | P(M_1, p_1) \rangle &= f_+(q^2) P_\mu + f_-(q^2) q_\mu, \\
\langle V(M_2, p_2, \epsilon) | V_\mu(0) | P(M_1, p_1) \rangle &= 2g(q^2) \epsilon_{\mu\nu\alpha\beta} \epsilon^{*\nu} p_1^\alpha p_2^\beta, \\
\langle V(M_2, p_2, \epsilon) | A_\mu(0) | P(M_1, p_1) \rangle &= i\epsilon^{*\alpha} [f(q^2) g_{\mu\alpha} + a_+(q^2) p_{1\alpha} P_\mu + a_-(q^2) p_{1\alpha} q_\mu], \\
\langle P(M_2, p_2) | T_{\mu\nu}(0) | P(M_1, p_1) \rangle &= -2i s(q^2) (p_{1\mu} p_{2\nu} - p_{1\nu} p_{2\mu}), \\
\langle V(M_2, p_2, \epsilon) | T_{\mu\nu}(0) | P(M_1, p_1) \rangle &= i\epsilon^{*\alpha} [g_+(q^2) \epsilon_{\mu\nu\alpha\beta} P^\beta + g_-(q^2) \epsilon_{\mu\nu\alpha\beta} q^\beta + g_0(q^2) p_{1\alpha} \epsilon_{\mu\nu\beta\gamma} p_1^\beta p_2^\gamma], \tag{1}
\end{aligned}$$

where $q = p_1 - p_2$, $P = p_1 + p_2$. The following notations are used: $\gamma^5 = i\gamma^0\gamma^1\gamma^2\gamma^3$, $\sigma_{\mu\nu} = \frac{i}{2}[\gamma_\mu, \gamma_\nu]$, $\epsilon^{0123} = -1$, $\gamma_5\sigma_{\mu\nu} = -\frac{i}{2}\epsilon_{\mu\nu\alpha\beta}\sigma^{\alpha\beta}$, and $Sp(\gamma^5\gamma^\mu\gamma^\nu\gamma^\alpha\gamma^\beta) = 4i\epsilon^{\mu\nu\alpha\beta}$. We study the form factors within the dispersion formulation of the quark model [16]. We start by considering the region $q^2 < 0$ where the form factors may be represented as double spectral representations in the invariant masses of the initial and final $q\bar{q}$ pairs. The form factors corresponding to the decay region $q^2 > 0$ are then derived by performing the analytical continuation.

The transition of the initial meson $q(m_2)\bar{q}(m_3)$ with the mass M_1 to the final meson $q(m_1)\bar{q}(m_3)$ with the mass M_2 induced by the quark transition $q(m_2) \rightarrow q(m_1)$ through the current $\bar{q}(m_1)O_\mu q(m_2)$ is described by the diagram of Fig.1. For constructing the double spectral representation we must consider a double-cut graph where all intermediate particles go on mass shell but the initial and final mesons have the off-shell momenta \tilde{p}_1 and \tilde{p}_2 such that $\tilde{p}_1^2 = s_1$ and $\tilde{p}_2^2 = s_2$ with $(\tilde{p}_1 - \tilde{p}_2)^2 = q^2$ kept fixed.

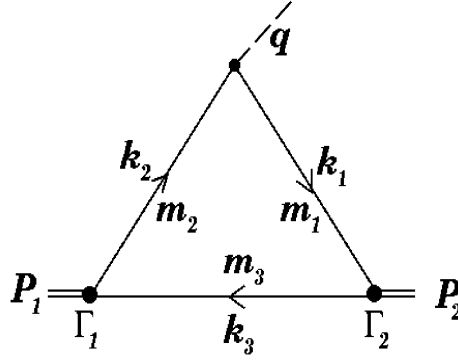


FIG. 1. One-loop graph for a meson decay.

The quark structure of the initial and final mesons is given in terms of the vertices Γ_1 and Γ_2 , respectively. The initial pseudoscalar meson vertex has the spinorial structure $\Gamma_1 = i\gamma_5 G_1/\sqrt{N_c}$; the final meson vertex has the structure $\Gamma_2 = i\gamma_5 G_2/\sqrt{N_c}$ for a pseudoscalar state and the structure $\Gamma_{2\mu} = [A\gamma_\mu + B(k_1 - k_3)_\mu] G_2/\sqrt{N_c}$, $A = -1$, $B = 1/(\sqrt{s_2} + m_1 + m_3)$ for an S -wave vector meson.

The double spectral densities \tilde{f} of the form factors are obtained by calculating the relevant traces and isolating the Lorentz structures depending on \tilde{p}_1 and \tilde{p}_2 . These invariant factors f account for the two-particle singularities in the Feynman graph.

For $q^2 < 0$ the spectral representations of the form factors have the form [16]

$$f_i(q^2) = \frac{1}{16\pi^2} \int_{(m_1+m_3)^2}^{\infty} ds_2 \varphi_2(s_2) \int_{s_1^-(s_2, q^2)}^{s_1^+(s_2, q^2)} ds_1 \varphi_1(s_1) \frac{\tilde{f}_i(s_1, s_2, q^2)}{\lambda^{1/2}(s_1, s_2, q^2)}, \tag{2}$$

where the wave function $\varphi_i(s_i) = G_i(s_i)/(s_i - M_i^2)$ and

$$s_1^\pm(s_2, q^2) = \frac{s_2(m_1^2 + m_2^2 - q^2) + q^2(m_1^2 + m_3^2) - (m_1^2 - m_2^2)(m_1^2 - m_3^2)}{2m_1^2} \pm \frac{\lambda^{1/2}(s_2, m_3^2, m_1^2)\lambda^{1/2}(q^2, m_1^2, m_2^2)}{2m_1^2}$$

and $\lambda(s_1, s_2, s_3) = (s_1 + s_2 - s_3)^2 - 4s_1s_2$ is the triangle function ². The analytical continuation of the expression (2) to the region $q^2 > 0$ gives the form factor at $q^2 \leq (m_2 - m_1)^2$. Explicit expressions of the double spectral densities of all the form factors in (1) and more details can be found in [16].

²The spectral densities \tilde{f} include proper subtraction terms. These subtraction terms have been determined in [16] by matching the structure of the heavy quark expansion in the quark model to the structure of the heavy-quark expansion in QCD

The soft wave function of a meson $M [q(m_q)\bar{q}(m_{\bar{q}})]$ can be written as follows

$$\varphi(s) = \frac{\pi}{\sqrt{2}} \frac{\sqrt{s^2 - (m_q^2 - m_{\bar{q}}^2)^2}}{\sqrt{s - (m_q - m_{\bar{q}})^2}} \frac{w(k^2)}{s^{3/4}} \quad (3)$$

with $k^2 = \lambda(s, m_q^2, m_{\bar{q}}^2)/4s$. Here the ground-state radial S -wave function $w(k^2)$ is normalized as $\int w^2(k^2)k^2 dk = 1$.

As demonstrated in [16] the form factors develop the correct structure of the heavy-quark expansion in accordance with QCD in the leading and next-to-leading $1/m_Q$ orders, if the radial wave functions $w(k^2)$ are localized in a region of the order of the confinement scale, $k^2 \lesssim \Lambda^2$. We assume a simple gaussian parametrization of the radial wave function

$$w(k^2) \propto \exp(-k^2/2\beta^2), \quad (4)$$

which satisfies the localization requirement for $\beta \simeq \Lambda_{QCD}$.

It is worth noting that the quark model describes the meson structure in terms of the constituent quarks whereas the weak currents are given in terms of the current quarks. Thus the form factor expression (2) should be multiplied by the constituent quark form factor $f_{q_2 \rightarrow q_1}(q^2)$ as follows

$$f_{M_1 \rightarrow M_2}(q^2) \rightarrow f_{q_2 \rightarrow q_1}(q^2) f_{M_1 \rightarrow M_2}(q^2). \quad (5)$$

The spectral representations (2) take into account long-distance contributions connected with the meson formation in the initial and final channels. At the same time the quantity $f_{q_2 \rightarrow q_1}(q^2)$ encodes additional long-distance effects in the q^2 channel. The form factor $f_{q_2 \rightarrow q_1}(q^2)$ contains poles at $q^2 = M_{\text{res}}^2$ but as shown in the analysis of the elastic meson form factors fastly goes to unity beyond the resonance region. In heavy-to-heavy quark transition, the form factor $f_{q_2 \rightarrow q_1}(q^2)$ is equal to unity within the $1/m_Q^2$ accuracy in the whole kinematical decay region. The particular form of the quark transition form factor does not depend on the initial and final mesons involved but rather depends on the set of the relevant hadronic resonances in the q^2 channel and is different for the vector, axial-vector etc channels. Numerically, in all modes but $B \rightarrow \pi$ (see [22]) the effect of the constituent quark form factor turns out to be negligible.

The leptonic decay constant of the pseudoscalar meson f_P is given in terms of its wave function by the spectral representation [16]

$$f_P = \sqrt{N_c}(m_q + m_{\bar{q}}) \int ds \varphi(s) \frac{\lambda^{1/2}(s, m_q^2, m_{\bar{q}}^2)}{8\pi^2 s} \frac{s - (m_q - m_{\bar{q}})^2}{s}. \quad (6)$$

III. PARAMETERS OF THE MODEL AND NUMERICAL RESULTS

A. Parameters of the model

We consider the slope parameter β of the meson wave function (4) and the constituent quark masses as fit parameters. The relevant values for the B , ρ , and π mesons have already been determined in [22] from a fit to the lattice results on the form factors $T_2(q^2)$ and $A_1(q^2)$ (see eq (9) below) at $q^2 = 19.6$ and 17.6 GeV^2 [14]. Thereby, use has been made of the spectral representation of the leptonic decay constant (6), and the double spectral representations (2) of the form factors. The values obtained for m_b , m_u , and β_B , β_ρ , β_π are displayed in Table I.

A few comments on these numbers are in order:

- The quark model double spectral representations take into account long-range QCD effects but not the short-range perturbative corrections. However, by fitting the wave functions and masses to reproduce the lattice points, these corrections are effectively taken care of: Corrections to the quark propagators correspond to the appearance of the effective quark masses. Corrections to the vertices at the relevant values of the recoil variable $\omega = (M_B^2 + m_\pi^2 - q^2)/2M_B M_\pi$ should be small as found in form factors of other meson transitions [24].
- The value obtained for the b -quark mass $m_b = 4.85 \text{ GeV}$ is close to the one-loop pole mass which in fact is the relevant mass for quark model calculations.

We now need to fix the parameters describing the strange and charmed mesons. The charm quark mass can be determined from the well-known $1/m_Q$ expansion of the heavy meson mass in terms of the heavy quark mass and the hadronic parameters $\bar{\Lambda}$, λ_1 and λ_2 . Using the recent estimates of these parameters one finds

$$m_b - m_c \simeq 3.4 \text{ GeV}. \quad (7)$$

This provides $m_c \simeq 1.45 \text{ GeV}$. For m_s one expects $m_s \simeq 350 - 370 \text{ MeV}$ taking into account that $m_u = 230 \text{ MeV}$.

A stringent way to constrain the parameters m_s , β_K , β_{K^*} , and β_D is provided by the measured integrated rates of the semileptonic decays $D \rightarrow (K, K^*)l\nu$. In addition we apply the relation (6) which connects β_K with m_s by using the known value of the K -meson leptonic decay constant $f_K = 160 \text{ MeV}$. The parameter values found this way are displayed in Table I³. The corresponding form factors and decay rates are given in Tables IV and VI.

The polarization of the K^* in the $D \rightarrow K^*l\nu$ decays turns out to be in good agreement with the experimental result (Table VI), and the calculated D meson decay constant $f_D = 200 \text{ MeV}$ corresponds to the expectation for the magnitude of this quantity.

The parameter β_D^* cannot be found this way, but it should be close to β_D because of the heavy quark symmetry requirements. We therefore set $\beta_{D^*} = \beta_D$.

Also listed in Table I are the parameters which describe strange heavy mesons. They are discussed in subsection D.

TABLE I. Constituent quark masses and slope parameters of the exponential wave function (in GeV).

m_u	m_s	m_c	m_b	β_π	β_K	β_D	β_B	β_{η_s}	β_{D_s}	β_{B_s}	β_ρ	β_{K^*}	β_{D^*}	β_ϕ
0.23	0.35	1.45	4.85	0.36	0.42	0.46	0.54	0.45	0.48	0.56	0.31	0.42	0.46	0.45

TABLE II. Leptonic decay constants of the pseudoscalar mesons in MeV calculated via 6 with the parameters of Table 1.

f_π	f_K	f_D	f_B	f_{η_s}	f_{D_s}	f_{B_s}
132	160	200	180	183	220	200

TABLE III. Meson masses in GeV from PDG [28]

M_π	M_K	M_η	$M_{\eta'}$	M_D	M_{D_s}	M_B	M_{B_s}	M_ρ	M_{K^*}	M_ϕ	M_{D^*}	$M_{D_s^*}$
0.14	0.49	0.547	0.958	1.87	1.97	5.27	5.97	0.77	0.89	1.02	2.01	2.11

The knowledge of the wave functions and the quark masses allows the calculation of the form factors. For convenience, we interpolate the numerical values of the form factors obtained by the spectral representation (2) according to a simple three-parameter formula

$$f(q^2) = f(0)/[1 - \sigma_1 q^2 + \sigma_2 q^4]. \quad (8)$$

The values of $f(0)$, σ_1 , and σ_2 are given for each decay mode in the relevant subsections.

We also present the often used dimensionless form factors V , A_1 , A_2 , A_3 , T_1 , T_3 [1] at $q^2 = 0$. They are given by the following linear combinations of the form factors of Eq. (1)⁴

$$\begin{aligned}
V &= (M_1 + M_2)g, & A_1 &= \frac{1}{M_1 + M_2}f, & A_2 &= -(M_1 + M_2)a_+, & A_0 &= \frac{1}{2M_2}(f + q^2 \cdot a_- + Pq \cdot a_+), \\
T_1 &= -\frac{1}{2}g_+, & T_2 &= -\frac{1}{2}(g_+ + \frac{q^2}{Pq}g_-), & T_3 &= \frac{1}{2}\frac{M_1 + M_2}{M_1 - M_2}\left(g_- - \frac{Pq}{2}g_0\right).
\end{aligned} \quad (9)$$

³In [23] a different set of the parameters was used which also provided a good description of the available experimental data on semileptonic B and D decays. However, the corresponding form factors have a rather flat q^2 -dependence and do not match the lattice results at large q^2 .

⁴Notice that P. Ball and V. Braun [11] use a different definition of T_i , namely: $T_{1,2} = T_{1,2}^{BB}/2$, and $T_3 = (M_1 + M_2)/(M_1 - M_2)T_3^{BB}/2$

B. Charmed meson decays

1. $D \rightarrow K, K^*$

The $D \rightarrow K, K^*$ decays are induced by the charged current $c \rightarrow s$ quark transition. As described in the previous section, the measured total rates of these decays are used for a precise fit of the parameters of our model. With the parameters of Table I we obtain the form factors listed in Table IV. Table V compares the form factors at $q^2 = 0$ with the results of other approaches and Table VI presents the decay rates.

TABLE IV. The $D \rightarrow K, K^*$ transition form factors.

	$D \rightarrow K$			$D \rightarrow K^*$						
	f_+	f_-	s	g	f	a_+	a_-	g_+	g_-	g_0
$f(0)$	0.78	-0.50	0.32	0.375	1.83	-0.177	0.36	-0.78	0.65	0.145
σ_1	0.278	0.34	0.28	0.28	0.059	0.148	0.26	0.276	0.31	0.42
σ_2	0.012	0.018	0.011	0.012	0.0043	0.01	0.012	0.0086	0.0023	0.05

TABLE V. Comparison of the results of different approaches for the semileptonic $D \rightarrow K, K^*$ form factors at $q^2 = 0$.

Ref.	$f_+(0)$	$V(0)$	$A_1(0)$	$A_2(0)$
This work	0.78	1.03	0.66	0.49
WSB [1]	0.76	1.3	0.88	1.2
Jaus'96 [4]	0.78	1.04	0.66	0.43
SR [9]	0.60(15)	1.10(25)	0.50(15)	0.60(15)
Lat(average) [13]	0.73(7)	1.2(2)	0.70(7)	0.6(1)
Exp [26]	0.76(3)	1.07(9)	0.58(3)	0.41(5)

TABLE VI. The $D \rightarrow (K, K^*)l\nu$ decay rates in $10^{10} s^{-1}$ obtained within different approaches, $|V_{cs}| = 0.975$.

Ref.	$\Gamma(D \rightarrow K)$	$\Gamma(D \rightarrow K^*)$	$\Gamma(K^*)/\Gamma(K)$	Γ_L/Γ_T
This work	9.7	6.0	0.63	1.28
Jaus'96 [4]	9.6	5.5	0.57	1.33
SR [9]	6.5(1.5)	3.8(1.5)	0.50(15)	0.86(6)
Exp [27]	9.3(4)	5.7(7)	0.61(7)	1.23(13) [28]

2. $D \rightarrow \pi, \rho$

These decays are induced by the $s \rightarrow u$ charged current. Since all the necessary parameters have already been fixed, this mode allows for a parameter-free prediction. Table VII presents the results of our calculations. In Tables VIII and IX we compare our results with different approaches and with experimental data. The form factors at $q^2 = 0$ are close to the predictions of the relativistic quark model of Ref. [4], but the q^2 dependence is different such that our model and [4] lead to different decay rates. Although the experimental errors are very large and nearly all theoretical results agree with experiment, we notice a perfect agreement of our decay rates with the central values.

TABLE VII. The calculated $D \rightarrow \pi, \rho$ transition form factors.

	$D \rightarrow \pi$			$D \rightarrow \rho$						
	f_+	f_-	s	g	f	a_+	a_-	g_+	g_-	g_0
$f(0)$	0.69	-0.47	0.3	0.34	1.56	-0.185	0.32	-0.65	0.51	0.134
σ_1	0.32	0.376	0.32	0.347	0.121	0.212	0.328	0.345	0.371	0.52
σ_2	0.015	0.019	0.015	0.019	-0.0023	0.014	0.019	0.019	0.0187	0.082

TABLE VIII. Comparison of the results of different approaches for the semileptonic $D \rightarrow \pi, \rho$ form factors at $q^2 = 0$.

Ref.	$f_+(0)$	$V(0)$	$A_1(0)$	$A_2(0)$
This work	0.69	0.89	0.6	0.49
WSB [1]	0.69	1.23	0.78	0.92
Jaus'96 [4]	0.67	0.93	0.58	0.42
SR [9]	0.50(15)	1.0(2)	0.5(2)	0.4(2)
Lat(ave) [13]	0.65(10)	1.1(2)	0.65(7)	0.55(10)

 TABLE IX. The $D \rightarrow (\pi, \rho) l \nu$ decay rates in $10^{10} s^{-1}$, $|V_{cd}| = 0.22$.

Ref.	$\Gamma(D \rightarrow \pi)$	$\Gamma(D \rightarrow \rho)$	$\Gamma(\rho)/\Gamma(\pi)$	Γ_L/Γ_T
This work	0.948	0.42	0.45	1.16
WSB [1]	0.68	0.67	1.0	0.91
Jaus'96 [4]	0.8	0.33	0.41	1.22
SR [9]	0.39(8)	0.12(4)	–	1.31(11)
Melikhov'97 [23]	0.62	0.26	0.41	1.27
Exp [29]	0.92(45)	0.45(22)	0.50(35)	–

C. Beauty meson decays

1. $B \rightarrow D, D^*$

These decays arise from the heavy-quark $b \rightarrow c$ transition. Here one has rigorous predictions for the expansion of the form factors in terms of the heavy-quark mass [18]. Namely, the main part of the form factors can be expressed through the universal form factor - the Isgur-Wise function. Different models provide different q^2 -dependences of the Isgur-Wise function as well as different subleading $1/m_Q$ corrections.

We recall that our spectral representations of the form factors explicitly respect the HQET predictions for the leading and the subleading orders of the heavy-quark expansion, so that we expect reliable predictions for the form factors. Our numerical results are summarized in Tables X, XI, and XII.

 TABLE X. The calculated $B \rightarrow D, D^*$ transition form factors.

	$B \rightarrow D$			$B \rightarrow D^*$						
	f_+	f_-	s	g	f	a_+	a_-	g_+	g_-	g_0
$f(0)$	0.667	-0.339	0.97	0.104	4.807	-0.085	0.098	-0.68	0.389	0.0052
σ_1	0.0404	0.041	0.0404	0.0406	0.019	0.0365	0.039	0.0407	0.0415	0.059
σ_2	0.00037	0.00036	0.00036	0.00037	-0.000035	0.0003	0.00034	0.00037	0.00038	0.00126

 TABLE XI. Comparison of the results of different approaches for the semileptonic $B \rightarrow D, D^*$ form factors at $q^2 = 0$.

Ref.	$f_+(0)$	$V(0)$	$A_1(0)$	$A_2(0)$	$A_0(0)$
This work	0.667	0.757	0.66	0.62	0.69
WSB [1]	0.61	0.71	0.65	0.69	0.62
Jaus'96 [4]	0.69	0.81	0.69	0.64	

TABLE XII. The $B \rightarrow (D, D^*)l\nu$ decay rates in $|V_{cb}|^2 ps^{-1}$.

Ref.	$\Gamma(B \rightarrow D)$	$\Gamma(B \rightarrow D^*)$	$\Gamma(D^*)/\Gamma(D)$	Γ_L/Γ_T
This work	8.57	22.82	2.66	1.11
Jaus'96 [4]	9.6	25.33	2.64	
Melikhov'97 [23]	8.7	21.0	2.65	1.28
Exp	$(1.34 \pm 0.15)10^{-2} ps^{-1}$ [32]	$(2.98 \pm 0.17)10^{-2} ps^{-1}$ [28]	2.35(1.3)	1.24(0.16) [33]

2. $B \rightarrow K, K^*$

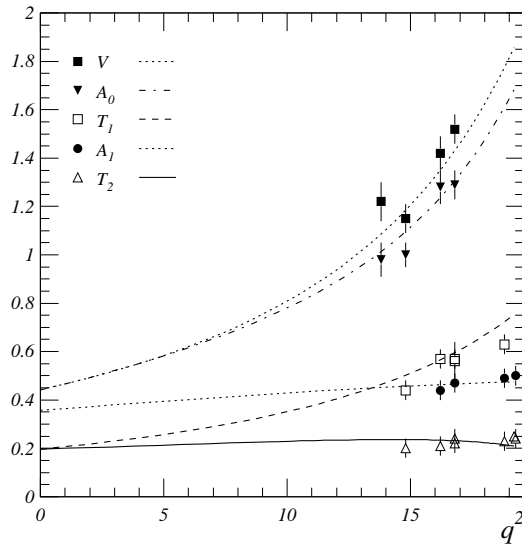
These decays are induced by the $b \rightarrow s$ Flavor Changing Neutral Current (FCNC). Notice that the $B \rightarrow \pi, \rho$ form factors at large q^2 have been used to fix the parameters of the model. Thus we expect that the predictions for the $B \rightarrow K, K^*$ form factors which in fact differ from the former mode only by SU(3) violating effects should be reliable. Table XIII presents the calculated form factors and Fig 2 gives our predictions together with the available lattice results at large q^2 . The good agreement shows that the size and the sign of the SU(3) violating effects are correctly accounted for.

 TABLE XIII. The calculated $B \rightarrow K, K^*$ transition form factors.

	$B \rightarrow K$			$B \rightarrow K^*$						
	f_+	f_-	s	g	f	a_+	a_-	g_+	g_-	g_0
$f(0)$	0.36	-0.29	0.06	0.072	2.2	-0.0525	0.061	-0.393	0.357	0.06
σ_1	0.05	0.051	0.28	0.051	0.0217	0.042	0.046	0.050	0.052	0.072
σ_2	0.00056	0.00058	0.011	0.00059	0.00042	0.00045	0.00052	0.00060	0.00062	0.0022

 TABLE XIV. Comparison of the results of different approaches for the $B \rightarrow K, K^*$ form factors at $q^2 = 0$.

Ref.	$f_+(0)$	$V(0)$	$A_1(0)$	$A_2(0)$	$A_0(0)$	$T_1(0)$	$T_3(0)$
This work	0.36	0.44	0.36	0.32	0.45	0.196	0.194
SR [10]	0.25	0.47	0.37	0.40	0.30	0.19	-
Lat+Stech [14]	-	0.38	0.28	-	0.32	0.16	-
LCSR'98 [11]	0.34	0.46	0.34	0.28	0.47	0.19	0.182


 FIG. 2. Form factors of the $B \rightarrow K^*$ transition vs the lattice results.

3. $B \rightarrow \pi, \rho$

These transitions have been used for determining the parameters of our quark model in the u, d and b sectors by fitting the quark-model form factors available lattice results on T_2 and A_1 at large q^2 . The corresponding form factors for all relevant q^2 are given in the dedicated paper [22] and we do not repeat them here. Instead, we compare the results obtained from the quark model of Ref. [22] with results of the quark model of Jaus [4] and latest light-cone sum rule (LCSR) results [11], see Table XV. One can see a very good agreement between the quark model of Jaus, LCSRs, and our approach. The only visible difference with the LCSR method is in the form factor $A_0(0)$, which is caused by small differences in $A_1(0)$ and $A_2(0)$ (recall that $A_0(0) = ((M_1 + M_2)A_1(0) - (M_1 - M_2)A_2(0)) / 2M_2$) The discrepancy does not much exceed the 15% error bar quoted for the LCSR results.

If the LCSR results at small q^2 and lattice results at large q^2 are correct, our approach does surely provide a realistic description of the form factors at all kinematically accessible q^2 values.

TABLE XV. Comparison of the results of different approaches on weak $B \rightarrow \pi, \rho$ form factors at $q^2 = 0$.

Ref.	$f_+(0)$	$V(0)$	$A_1(0)$	$A_2(0)$	$A_0(0)$	$T_1(0)$	$T_3(0)$
This work	0.285	0.31	0.225	0.24	0.29	0.135	0.132
Jaus'96 [4]	0.27	0.35	0.26	0.24	-	-	-
LCSR'98 [11]	0.305	0.34	0.26	0.22	0.37	0.14	0.134

Summing up our results on the decays of the nonstrange heavy mesons, we found no disagreement neither with the existing experimental data nor with the available results of the lattice QCD or sum rules in their specific regions of validity.

In the next section we apply our model to the decay of strange heavy mesons for which a few new parameters have to be introduced which are specific for the description of the weak decays of strange heavy mesons to light mesons.

D. Decays of the strange mesons D_s and B_s

For dealing with these decays, we must first specify the slope parameters of the B_s and the D_s wave function. We obtain them by applying (6) and using $f_{B_s}/f_B = 1.1$ and $f_{D_s}/f_D = 1.1$ in agreement with the lattice estimates for these values [13]. The resulting values of the slope parameters are listed in Table I. For most of the modes all other parameters have already been fixed, such that we can directly calculate the form factors. The only exception are the decays into the η, η', ϕ final states. For their treatment we need to know the ϕ wave function, the mixing angle and the slope of the radial wave function of the $s\bar{s}$ component in η and η' . Our procedure of fixing these parameters are discussed in the relevant subsection.

1. $D_s \rightarrow K, K^*$

These meson transition are driven by the charged-current $c \rightarrow d$ quark transition. The results of the calculation are given in Tables XVI and XVII, and the prediction for the rates of the semileptonic decays are displayed in Table XVIII.

TABLE XVI. The calculated $D_s \rightarrow K, K^*$ transition form factors.

	$D_s \rightarrow K$			$D_s \rightarrow K^*$						
	f_+	f_-	s	g	f	a_+	a_-	g_+	g_-	g_0
$f(0)$	0.72	-0.58	0.31	0.365	1.64	-0.146	0.35	-0.712	0.706	0.165
σ_1	0.30	0.37	0.30	0.30	0.0708	0.12	0.28	0.30	0.348	0.45
σ_2	0.0125	0.024	0.011	0.0125	0.0255	0.0166	0.017	0.0128	0.0153	0.0607

TABLE XVII. The $D_s \rightarrow K, K^*$ transition form factors at $q^2 = 0$.

Ref.	$V(0)$	$A_1(0)$	$A_2(0)$	$A_0(0)$	$T_1(0)$	$T_3(0)$
This work	1.044	0.57	0.42	0.67	0.36	0.6

TABLE XVIII. The $D_s \rightarrow (K, K^*)l\nu$ decay rates in $10^{10} s^{-1}$, $|V_{cd}| = 0.22$.

Ref	$\Gamma(D_s \rightarrow K)$	$\Gamma(D_s \rightarrow K^*)$	$\Gamma(K^*)/\Gamma(K)$	Γ_L/Γ_T
This work	0.63	0.38	0.6	1.21

2. $D_s \rightarrow \eta, \eta', \phi$

These decay modes are induced by the charged current $c \rightarrow s$ quark transition. The pseudoscalar mesons η and η' are mixtures of the nonstrange and the strange components with the flavour wave functions $\eta_n \equiv \frac{\bar{u}u + \bar{d}d}{\sqrt{2}}$ and $\eta_s = \bar{s}s$, respectively,

$$\begin{aligned}\eta &= \cos(\varphi) \eta_n - \sin(\varphi) \eta_s \\ \eta' &= \sin(\varphi) \eta_n + \cos(\varphi) \eta_s,\end{aligned}\tag{10}$$

with the angle $\varphi \simeq 40^\circ$ [34,35]. The decay rates of interest are

$$\begin{aligned}\Gamma(D_s \rightarrow \eta l\nu) &= \sin^2(\varphi) \Gamma(D_s \rightarrow \eta_s (M_\eta) l\nu) \\ \Gamma(D_s \rightarrow \eta' l\nu) &= \cos^2(\varphi) \Gamma(D_s \rightarrow \eta_s (M_{\eta'}) l\nu).\end{aligned}\tag{11}$$

Let us give a brief explanation of these formulas: The semileptonic decay rates are determined by the form factor f_+ . The spectral representation of this form factor does not involve the final meson mass explicitly. This means that for the $\bar{s}s$ component of both η and η' we have to deal with the same form factor, which can be expressed through the radial wave function of this component. On the other hand, the phase-space volume of the decay process is determined by the physical meson masses, as indicated in (11). It should be clear, however, that the η_s is not an eigenstate of the Hamiltonian and thus does not have any definite mass.

Assuming universality of the wave functions of the ground state pseudoscalar 0^- nonet, the radial wave function of the nonstrange component Ψ_{η_n} coincides with the pion radial wave function [34]. The radial wave function Ψ_{η_s} should be determined independently. From the analysis of a broad set of processes the leptonic decay constant f_s of the strange component η_s , has been found to lie in the interval $f_s = (1.36 \pm 0.04) f_\pi$ [35]. This allows us to determine the slope parameter β_{η_s} in such a way that the calculated value of f_s lies in this interval, and the calculated ratio $\Gamma(D_s \rightarrow \eta)/\Gamma(D_s \rightarrow \eta')$ agrees with the experimental data for $\varphi = 40^\circ$. This procedure yields for the slope parameter $\beta_{\eta_s} = 0.45$ ⁵. For the slope parameter β_ϕ of the wave function of the ϕ -meson, which is the vector $\bar{s}s$ state, we expect a value close to β_{η_s} .

In fact, $\beta_\phi = 0.45 \text{ GeV}$ leads to the $B_s \rightarrow \phi$ transition form factors which agree well with the LCSR results at $q^2 = 0$ (see subsection 4). With all other quark model parameters fixed from the description of the nonstrange heavy meson decays and taking a simple Gaussian form of the radial wave function, the decay rate $\Gamma(D_s \rightarrow \phi l\nu)$ is a function of β_ϕ . This function has a minimum at the value $\beta_\phi = 0.45 \text{ GeV}$; nevertheless, the corresponding value of the decay rate is 1σ above the central experimental value).

The results of our calculations are given in Tables XIX, XX, and XXI.

 TABLE XIX. The calculated $D_s \rightarrow \eta_s, \phi$ transition form factors.

	$D_s \rightarrow \eta_s$			$D_s \rightarrow \phi$						
	f_+	f_-	s	g	f	a_+	a_-	g_+	g_-	g_0
f(0)	0.784	-0.56	0.32	0.372	1.93	-0.157	0.36	-0.77	0.68	0.153
σ_1	0.275	0.346	0.28	0.28	0.0758	0.128	0.26	0.278	0.32	0.415
σ_2	0.0105	0.022	0.0097	0.0108	0.0093	0.0134	0.0146	0.0109	0.0081	0.05

⁵Another procedure of taking into account the SU(3) breaking effects to obtain Ψ_{η_s} from Ψ_{η_n} has been proposed in [34].

TABLE XX. The $D_s \rightarrow \phi$ transition form factors at $q^2 = 0$.

Ref.	$V(0)$	$A_1(0)$	$A_2(0)$	$A_0(0)$	$T_1(0)$	$T_3(0)$
This work	1.11	0.65	0.47	0.73	0.39	0.73

 TABLE XXI. The $D_s \rightarrow (\eta, \eta', \phi)l\nu$ decay rates in $10^{10} s^{-1}$, $|V_{cs}| = 0.975$. The experimental rates are obtained from the corresponding branching ratios using the D_s lifetime $\tau_{D_s} = 0.495 \pm 0.013 ps$ from the 1999 update [28]

Ref	$\Gamma(D_s \rightarrow \eta)$	$\Gamma(D_s \rightarrow \eta')$	$\Gamma(D_s \rightarrow \phi)$
This work	5.0	1.85	5.1
Exp [28]	5.2 ± 1.3	2.0 ± 0.8	4.04 ± 1.01

3. $B_s \rightarrow K, K^*$

This mode is driven by the $b \rightarrow u$ charged current transition. The only additional new parameter needed here is the slope of the B_s wave function. We obtain it by using (6) and taking $f_{B_s}/f_B = 1.1$. The results of our calculation are given in Table XXII.

 TABLE XXII. The calculated $B_s \rightarrow K, K^*$ transition form factors.

	$B_s \rightarrow K$			$B_s \rightarrow K^*$						
	f_+	f_-	s	g	f	a_+	a_-	g_+	g_-	g_0
$f(0)$	0.31	-0.27	0.054	0.06	1.83	-0.042	0.051	-0.32	0.31	0.0058
σ_1	0.0547	0.056	0.0542	0.056	0.0267	0.047	0.0508	0.056	0.057	0.077
σ_2	0.00073	0.00095	0.0007	0.00077	0.000585	0.00073	0.00087	0.00076	0.0008	0.0029

The form factors at $q^2 = 0$ are compared with the LCSR predictions in Table XXIII. We observe some disagreement between our predictions and the LCSR calculation which gives smaller values for all the form factors. A closer look at the origin of this discrepancy shows that the only source is the strength and sign of the SU(3)-breaking effects. They lead to opposite corrections in the two approaches.

 TABLE XXIII. Comparison of the QM and LCSR results on the $B_s \rightarrow K, K^*$ form factors at $q^2 = 0$.

Ref.	$f_+(0)$	$V(0)$	$A_1(0)$	$A_2(0)$	$A_0(0)$	$T_1(0)$	$T_3(0)$
This work	0.31	0.38	0.29	0.265	0.37	0.16	0.16
LCSR'98 [11]	-	0.262	0.19	0.164	0.254	0.11	0.112

 TABLE XXIV. The $B_s \rightarrow (K, K^*)l\nu$ decay rates in $|V_{ub}|^2 10^{12} s^{-1}$.

Ref	$\Gamma(B_s \rightarrow K)$	$\Gamma(B_s \rightarrow K^*)$	Γ_L/Γ_T
This work	32.0	34.5	0.28

To discuss these SU(3) breaking effects, let us start with $B \rightarrow \rho$, which in fact differs from the $B_s \rightarrow K^*$ only by the flavour of the spectator quark, and move to $B_s \rightarrow K^*$ by accounting for the SU(3) violating effects:

Within the LCSR method there are two changes which affect the form factors: first, the change $f_{B_s} \rightarrow f_B$ leads to an increase of the $B_s \rightarrow K^*$ form factors; second, the change of the symmetric twist-two distribution amplitude of the ρ -meson to the asymmetric one of the K^* meson leads to a decrease of the form factors. The second effect turns out to be much stronger than the first one with the result of an overall decrease of the form factors.

In the quark model, the same SU(3) breaking effects take place: The change of the spectator mass (it determines the increase of f_{B_s}/f_B) and the change of the K^* meson wave function (due to the change of both the quark mass and the slope parameter of the light meson wave function); the influence of the slope of the heavy meson wave function upon the form factor is only marginal. Here the resulting effect of these changes leads to an increase of the form factors.

We want to point out that the difference between the results of the two approaches does not arise from specific effects (higher twists, higher radiative corrections etc) which are present in the LCSRs but absent in the quark model. The observed difference is purely due to the different strength of the SU(3) violating effects at the level of the twist-2 distribution amplitude. As was discussed in [24], this distribution amplitude can be expressed through the radial soft wave function of the meson. The mentioned SU(3) violating change of the quark-model wave function do not induce a strong asymmetry of the leading twist-2 distribution amplitude.

In view of the discrepancy between our results and the LCSR it would be interesting to have independent calculations of the $B_s \rightarrow K^*$ form factors at small q^2 from the 3-point sum rules, as well as a lattice calculation for large q^2 .

4. $B_s \rightarrow \eta, \eta', \phi$

These weak meson transitions are induced by the FCNC $b \rightarrow s$ quark transition. The results of the form factor calculation are given in Table XXV and compared with the LCSR predictions at $q^2 = 0$ in Table XXVI. The agreement between the two values is satisfactory at least within the declared 15% accuracy of the LCSR predictions. This allows us to expect that also the $D_s \rightarrow \phi, \eta, \eta'$ form factors and the corresponding decay rates (section 2) are calculated reliably.

TABLE XXV. The calculated $B_s \rightarrow \eta_s, \phi$ transition form factors.

	$B_s \rightarrow \eta_s$			$B_s \rightarrow \phi$						
	f_+	f_-	s	g	f	a_+	a_-	g_+	g_-	g_0
$f(0)$	0.356	-0.30	0.061	0.069	2.18	-0.048	0.059	-0.38	0.35	0.0065
σ_1	0.052	0.054	0.052	0.053	0.025	0.044	0.049	0.053	0.0546	0.073
σ_2	0.00067	0.00085	0.00065	0.0007	0.00049	0.000615	0.0007	0.00069	0.00073	0.0025

TABLE XXVI. Comparison of the QM and LCSR results on the $B_s \rightarrow \phi$ form factors at $q^2 = 0$.

Ref.	$f_+(0)$	$V(0)$	$A_1(0)$	$A_2(0)$	$A_0(0)$	$T_1(0)$	$T_3(0)$
This work	0.31	0.44	0.34	0.31	0.42	0.19	0.19
LCSR'98 [11]	-	0.433	0.296	0.255	0.382	0.174	0.187

IV. CONCLUSION

We have calculated numerous form factors of heavy meson transitions to light mesons which are relevant for the semileptonic (charged current) and penguin (flavor-changing neutral current) decay processes. Our approach is based on evaluating the triangular decay graph within a relativistic quark model which has the correct analytical properties and satisfies all general requirements of QCD.

The model connects different decay channels in a unique way and gives the form factors for all relevant q^2 values. The disadvantage of the constituent quark model, namely its dependence on ill-defined parameters such as the effective constituent quark masses, have been greatly diminished by using several constraints: the quark masses and the slope parameters of the wave functions are chosen such that the calculated form factors reproduce the lattice results for the $B \rightarrow \pi, \rho$ form factors at large q^2 and the observed integrated rates of the semileptonic $D \rightarrow K, K^*$ decays.

Our main results are as follows:

- In spite of the rather different masses and properties of mesons involved in weak transitions, all existing data on the form factors, both from theory and experiment, can be understood in our quark picture. Namely, all the form factors are essentially described by the few degrees of freedom of constituent quarks, i.e. their wave functions and their effective masses. Details of the soft wave functions are not crucial; only the spatial extension of these wave functions of order of the confinement scale is important. In other words, only the meson radii are essential.
- The calculated transition form factors are in all cases in good agreement with the results available from lattice QCD and from sum rules in their specific regions of validity. The only exception is a disagreement with the LCSR results for the $B_s \rightarrow K^*$ transition where we predict larger form factors. This disagreement is caused by

a different way of taking into account the SU(3) violating effects when going from $B \rightarrow \rho$ to $B_s \rightarrow K^*$ and is not related to specific details of the dynamics of the decay process. We suspect that the LCSR method overestimates the SU(3) breaking in the long-distance region but this problem deserves further clarification.

We cannot provide for definite error estimates of our predictions because of the approximate character of the constituent quark model. However from the fine agreement obtained in cases where checks are possible, we believe that the actual accuracy of our predictions for the form factors is around 10%. Since some parameters have been fixed by using lattice results and have also been tested using the sum rule predictions, further improvements of the accuracy of our predictions will follow if these approaches attain smaller errors. Of course, each precisely measured decay will also allow a more accurate determination of the parameters of the model and thus can be used to diminish the errors at least for closely related decays.

V. ACKNOWLEDGMENTS

We are grateful to M. Beyer, A. Le Yaouanc, N. Nikitin, O. Pène, and S. Simula for helpful and interesting discussions. One of us (DM) gratefully acknowledges the financial support of the Alexander von Humboldt Stiftung.

-
- [1] M. Wirbel, B. Stech, and M. Bauer, Z.Phys. C **29**, 637 (1985).
 - [2] N. Isgur, D. Scora, B. Grinstein, and M. Wise, Phys. Rev. D **39**, 799 (1989).
 - [3] D. Scora and N. Isgur, Phys. Rev. D **52**, 2783 (1995).
 - [4] W. Jaus, Phys. Rev. D **41**, 3394 (1990); D **53**, 1349 (1996).
 - [5] M. Neubert, V. Rieckert, B. Stech, and Q. P. Xu, in *Heavy Flavours*, First Edition, ed. by A.J. Buras, M. Lindner (World Scientific, Singapore, 1992), p. 286.
 - [6] R. Aleksan, A. Le Yaouanc, L. Oliver, O. Pène, and J.-C. Raynal, Phys. Rev. D **51**, 6235 (1995).
 - [7] R. N. Faustov and V. O. Galkin, Z. Phys. C **66**, 119 (1995).
 - [8] I. L. Grach, I. M. Narodetskii and S. Simula, Phys. Lett. B **385**, 317 (1996).
 - [9] P. Ball, V. Braun, and H. Dosch, Phys. Rev. D **44**, 3567 (1991); P. Ball, Phys. Rev. D **48**, 3190 (1993).
 - [10] P. Colangelo *et al.*, Phys. Rev. D **53**, 3672 (1996).
 - [11] P. Ball and V. M. Braun, Phys. Rev. D **58**, 094016 (1998); P. Ball, JHEP09, 005 (1998).
 - [12] V. M. Braun, e-print archive hep-ph/9911206 (1999) and references therein.
 - [13] J. M. Flynn and C. T. Sachrajda, e-print archive hep-lat/9710057 and references therein.
 - [14] UKQCD Collaboration, L. Del Debbio *et al*, Phys. Lett. B **416**, 392 (1998).
 - [15] B. Stech, Phys. Lett. B **354**, 447 (1995); Z. Phys. C **75**, 245 (1997).
 - [16] D. Melikhov, Phys. Rev. D **53**, 2460 (1996); D **56**, 7089 (1997).
 - [17] N. Isgur and M. B. Wise, Phys. Lett. B **232**, 113 (1989); Phys. Lett. B **237**, 527 (1990);
 - [18] M. Luke, Phys. Lett. B **252**, 447 (1990); M. Neubert and V. Rieckert, Nucl. Phys. B **382**, 97 (1992).
 - [19] N. Isgur and M. B. Wise, Phys. Rev. D **42**, 2388 (1990).
 - [20] J. Charles *et al*, Phys. Rev. D **60**, 014001 (1999).
 - [21] D. Melikhov, N. Nikitin, and S. Simula, Phys. Rev. D **57**, 6814 (1997).
 - [22] M. Beyer and D. Melikhov, Phys. Lett. B **436**, 344 (1998).
 - [23] D. Melikhov, Phys. Lett. B **394**, 385 (1997).
 - [24] V. Anisovich, D. Melikhov, and V. Nikonov, Phys. Rev. D **52**, 5295 (1995).
 - [25] I. Bigi, M. Shifman, N. Uraltsev, hep-ph/9307290 (1997).
 - [26] A. Ryd, Talk given at 7-th Int. Symp. on heavy Flavours, Santa barbara, California, July 1997.
 - [27] CLEO Collaboration, A. Bean *et al.*, Phys. Lett. B **317**, 647 (1993).
 - [28] Particle Data Group, C. Caso *et al*, EPJ C **3**, 1 (1998); 1999 partial update for edition 2000, URL: <http://pdg.lbl.gov>.
 - [29] The rates for the $D \rightarrow \pi$ and $D \rightarrow \rho$ are obtained by combining the values for the $D \rightarrow K$ and $D \rightarrow K^*$ with the measurements of the ratios of the branching fractions $D \rightarrow \pi/D \rightarrow K$ by CLEO [30] and $D \rightarrow \rho/D \rightarrow K^*$ by E653 [31].
 - [30] CLEO Collaboration, F. Butler *et al.*, Phys. Rev. D **52**, 2656 (1995).
 - [31] E653 Collaboration, K. Kodama *et al.*, Phys. Lett. B **316**, 455 (1993).
 - [32] CLEO Collaboration, J. Bartelet *et al.*, Phys. Rev. Lett. **82**, 3746 (1999).
 - [33] CLEO Collaboration, S. Sanghera *et al.*, Phys. Rev. D **47**, 791 (1993).
 - [34] V. Anisovich, D. Melikhov, and V. Nikonov, Phys. Rev. D **55**, 2918 (1997).
 - [35] Th. Feldmann, P. Kroll and B. Stech, Phys. Rev. D **58**, 114006 (1998).